ABS ACTA BIOLOGICA SIBIRICA
A journal on the biodiversity of Siberia and the adjacent lands

Acta Biologica Sibirica 12: 119–132 (2026)
doi: 10.5281/zenodo.18596034
http://journal.asu.ru

RESEARCH ARTICLE

DNA Cytometry Image Analysis Software

Maxim G. Kutsev[1], Roman N. Panarin[1], Michael V. Skaptsov[1], Kseniya K. Ryabova[2, 3], Olga V. Uvarova[1], Anastasia M. Koltunova[1]

1 *Altai State University, 61 Lenin Ave., Barnaul, 656049, Russian Federation*
2 *Siberian Federal University, 79 Svobodny Pr., Krasnoyarsk, 660041, Russian Federation*
3 *Federal Research Center "Krasnoyarsk Science Center of the Siberian Branch of the Russian Academy of Sciences", Akademgorodok, 50, Krasnoyarsk, 660036, Russian Federation*

Corresponding author: Maxim G. Kutsev (m_kucev@mail.ru)

Academic editor: R. Yakovlev | Received 7 January 2026 | Accepted 2 February 2026 | Published 12 February 2026

http://zoobank.org/5A94FC1A-6891-4046-9415-7CCA64804778

Citation: Kutsev MG, Panarin RN, Skaptsov MV, Ryabova KK, Uvarova OV, Koltunova AM (2026) DNA Cytometry Image Analysis Software. Acta Biologica Sibirica 12: 119–132. https://doi.org/10.5281/zenodo.18596034

Abstract

The article presents the development of BioDecod, a tool for the automated detection and quantification of cell nuclei in images. BioDecod enables accurate nuclei identification and counting, measurement of their fluorescence intensity, and generation of structured data. This Windows-based application developed in TypeScript has user-friendly interface and a minimal number of adjustable parameters. In comparison with ImageJ and CellProfiler, BioDecod simplifies the analysis workflow by allowing users to work within a single window, visualize changes in real-time, and process up to 100 images simultaneously. The analysis algorithm involves image segmentation via adaptive thresholding to identify nuclei, size-based filtering, and calculation of integral fluorescence parameters across four channels, with subsequent data export to Excel. Data visualization is implemented through scatter plots and histograms, featuring functionality for population gating and automatic statistical calculations. A comparative analysis of BioDecod and ImageJ demonstrated the superior efficiency of BioDecod in image processing, evidenced by a lower coefficient of variation (CV) – 6.31–7.69 % versus 14.26–31.1 %. This improvement is attributed to BioDecod's effective filtering of particle populations to exclude artifacts and image overlaps. BioDecod was validated using real-world samples – plants with genome sizes ranging from 0.45 to 64.54 pg. In summary, BioDecod provides a comprehensive solution for the acquisition and analysis of cell nucleus images, combining ease of use, configurable flexibility, and measurement precision, which makes it a valuable tool for researchers in the field of image cytometry.

Keywords
BioDecod, cell nuclei, DNA image cytometry, fluorescence, genome size, image segmentation, ImageJ, ploidy, plants

Introduction

Modern cytogenetic research is going through a significant technological leap, especially in the field of cell staining and subsequent visualization. For these purposes, fluorescence microscopy is widely used, which makes it possible to study cell structure in detail, as well as flow cytometry, which provides fast and accurate analysis of a large number of cells.

The key task of analyzing the data is to accurately identify and count the fluorescent signals emitted by cell nuclei stained with special dyes. These signals carry information about the ploidy of cells and the size of the genome, which is crucial for understanding the genetic characteristics of the studied samples. One of the promising techniques or studying genome sizes and ploidy levels is image cytometry, which combines ease of implementation compared to direct chromosome counting and the availability of equipment for small laboratories compared to flow cytometry.

However, standard software solutions for image analysis often prove to be insufficiently effective in processing complex biological data obtained in cytogenetics. This is due to the specific features of biological images, such as the heterogeneity of coloring, the overlap of objects and the presence of noise (Montazerinezhad et al. 2020).

In this regard, an urgent task is the search for or development of specialized software tools capable of efficiently and accurately analyzing images obtained in cytogenetic studies. Such programs should have advanced capabilities for image processing, automatic object identification, and statistical data analysis, which will significantly increase the effectiveness and reliability of such studies.

From the point of view of solving a wide range of scientific issues and applications that are used in biology and biomedical research, segmentation and analysis of cell microstructures are a universal technique for processing results of microscopy (Vu et al. 2019). In a typical analysis, individual cells or their compartments are recognized in images or, to increase statistical significance, in a series of images. Measurements may include various morphological indicators of cell images, including their relative intensity, size, shape, perimeter, texture features, and other parameters that indicate the status of cells, such as whether the cell has undergone differentiation, mitosis, apoptosis, quiescence, senescence (Chen et al. 2024). Important scopes of application of image analysis of cell nuclei are cancer screening (Li et al. 2024), detection of plant ploidy levels for breeding purposes and detection of hybridization processes (Kutsev et al. 2024), detection of diseases of domestic animals (Kellogg et al. 2024), detection of drug toxicity in vivo (Xu et al. al. 2023).

One of the problems of image cytometry is the unavailability of software and the lack of universal algorithms of data processing. However, the general sequence of actions for different software is similar and generally consists of the following steps: image segmentation (extraction of target elements in the image); analysis of parameters (integral brightness, uneven structure of objects, curvature of borders, ratio of geometric dimensions, etc.), selection of target data by the user (removal of artifacts and noise); statistical processing of target data (calculation of means, coefficient of variation, etc.). There are a few commercial programs, most often adapted by the manufacturer to work with specific equipment.

All programs can be divided into 4 groups according to the terms of access, autonomy, and programming language (Wiesmann et al. 2015). Tool Group I – stand-alone tools. This group consists of stand-alone tools dedicated to the assessment and segmentation of micrographs with an intuitive graphical interface and filters for preprocessing in manual, interactive, automated modes and is represented by Icy, CellProfiler, Daime, and ColorSeg. Tool Group II – Matlab-based tools. The second group is written in the Matlab scripting language, which includes BlobFinder and CellSegmenter. Both packages have a clear graphical interface with specialized segmentation functions. They offer great functionality and are extendible. Tool Group III – ImageJ-based tools. The third group unites the ImageJ and the ImageJ-based tools MiToBo and Fiji. All three offer great functionality and can be extended by writing additional modules, scripts, and macros. Tool Group IV – free demo versions of commercial tools. The fourth group covers free demo and trial versions of commercial image processing tools with limited functionality. This group includes Volocity Demo, AxioVision LE, and LAS AF Lite. Tool Group V – data sharing tools. The fifth group combines image analysis tools with a web-based client-server architecture and focuses on the organization, assessment, and distribution of image data. They provide web tools for manual segmentation and analysis of fluorescent micrographs. The group consists of Omero and Bisque.

One of the modern free programs for processing microscopic images is the SCIP (Scalable Cytometry Image Processing) package (Lippeveld et al. 2024). This software allows you to implement image profiling processes, illumination correction (to mitigate the influence of non-homogeneous illumination), and image segmentation. The big disadvantage of SCIP is the lack of a graphical interface and the ability to work only through the command line, which is a barrier for untrained users unfamiliar with distributed computing.

One of the successful applications for microscopic image processing is BlobFinder (Allalou et al. 2009). Unfortunately, it is not currently supported by developers. BlobFinder can batch process image data and quantify and localize cells and point signals in fluorescence microscopy images obtained using FISH, intercalator staining in a fast and simple way.

CellProfiler should also be mentioned among modern free programs. This is an open-source program for quantitative analysis of biological images that allows researchers without special knowledge in computer vision or programming to auto-

matically perform measurements and phenotyping on large sets of images (Stirling et al. 2021).

But the most widely used package is ImageJ used in medical research to evaluate cell apoptosis (Helmy et al. 2012) and other microscopy applications (Collins 2007). ImageJ is an open-source program, and a large number of macros have been developed for it to make it easier for untrained users (Fontenete et al. 2016).

Materials and methods

In this paper, we present a software tool for processing large-scale datasets of biovisualization, BioDecod (Panarin et al. 2024). This software allows you to process both ICM (Image Cytometry) datasets obtained using specialized equipment and fluorescence microscopy. During the processing, segmentation based on threshold values, which provides functions for setting segmentation parameters, calculating area, object asymmetry, integral brightness, its standard deviation, coefficient of variation, and arithmetic mean value for all analyzed objects, is used.

BioDecod provides export of final and intermediate data in tabular format (.CSV) for further processing in Microsoft Excel-compatible editors. The results can also be exported as graphical files of histograms and dotted diagrams. The source files for processing can be represented by 8-16 bit color and monochrome images in TIFF, JPG, JPEG, PNG formats, obtained using matrices in microscope cameras, as well as ICM – CMOS and CCD devices with a resolution of 2–16 megapixels.

In parallel, image processing was performed using the ImageJ program, a Fuji package for Windows (Broeke et al. 2015.) to compare the convenience and quantitative indicators of processing results.

To obtain the images, we used an ICM device prototype developed by us, which is an inverted fluorescence microscope with a 3.5X planachromatic lens, 450-490 nm LED fluorescence excitation, a 510 nm cut-off light filter for the green spectrum, 560 nm for the red spectrum, and a SONY CMOS image sensor with a resolution of 5 megapixels. In parallel, a micrograph was taken to compare the effect of the equipment on the result obtained using an Axio imager 2 fluorescence microscope (Zeiss, Germany) equipped with an Axiocam 506 Color CCD camera (Zeiss, Germany) with a resolution of 6 megapixels and a digitization depth of 16 bits. A 5X lens, an exciting light filter of 470 ± 20 nm, and an emission light filter of 525 ± 25 nm were used to photograph green fluorescent particles. A 5X lens, an exciting light filter of 545 ± 12 nm, and an emission light filter of 605 ± 35 nm were used for photographing red fluorescent particles and DNA cytometry.

To compare the results of ICM and flow cytometry, a CytoFLEX cytometer (Beckman Coulter Inc., USA) with a 488 nm excitation laser and a 585 nm cut-off light filter for green fluorescent particles and 610 nm for red fluorescent particles and DNA cytometry was used.

The analyzed objects were Red-fluo Microspheres fluorescent particles with 532 nm excitation wavelength and 588 nm radiation wavelength and Green-fluo Microspheres with 488 nm excitation wavelength and 518 nm radiation wavelength (Yuan Biotech, China), with a size of 5 microns, used, among others, for calibration of flow cytometers. According to the manufacturer's characteristics, the variability of the fluorescence intensity of the particles is up to 5 %. Before analysis, the suspension of fluorescent particles was diluted with distilled water 1 : 500.

For DNA cytometry, we used young intact leaves of Garden Strawberries (cv. 'Rumba'), Black Rice (cv. 'Aroma D Black rice'), Tomatoe (cv. 'Stupichke'), Corn (cv. 'Owatonna'), Rye (cv. 'Tatiana' and cv. 'Sibir'), Winter Wheat (cv. unknown), and *Allium tuberosum* L. The isolation and propidium iodide staining of nuclei for cytometry were carried out in accordance with a previously developed protocol (Skaptsov et al. 2024).

Results and discussion

We have investigated two use cases for the BioDecod application: with digital images obtained using the prototype we developed, and photographs obtained by a fluorescence microscope. The results of flow cytometry were used as control data for comparing measurement parameters.

BioDecod is a tool designed to automatically detect and quantify cell nuclei in images. Its key task is the accurate identification and counting of nuclei, as well as the measurement of their fluorescence parameters. As a result, we obtained a structured data file containing all the quantitative indicators.

The BioDecod software, developed for the Microsoft Windows operating system using the TypeScript programming language, is user-friendly and minimizes the number of necessary parameters. Compared to its analogues, BioDecod requires less manual data entry, which greatly simplifies the analysis process. So, to obtain the results of the average integral brightness of objects in an image in ImageJ, it is necessary to work in five program windows, for CellProfiler – in three. At the same time, neither ImageJ nor CellProfiler provide a distribution histogram with the ability to isolate a population of nuclei, followed by automatic calculation of statistics for a user-selected interval. Unlike them, BioDecod provides operations in a single window and allows you to display changes of the final result in real time, depending on the initial settings. The development of BioDecod takes into account the recommendations of end users, which made it possible to create a software product that is intuitive and maximally tailored to the needs of researchers.

The analysis process begins with image segmentation to highlight target objects (calibration particles or cell nuclei). Adaptive threshold processing is used to separate the image of objects from the background. This method automatically determines the optimal threshold values to minimize the variance between the foreground and background of the image. The user sets initial thresholds for the bright-

ness, color, and area of objects (Fig. 1a), based on which the objects are outlined (Fig. 2b).

After identifying each object, BioDecod determines and assigns a brightness level to it. At the preprocessing stage, the images of the nuclei are filtered according to the size by the user, which eliminates overlapping images and artifacts. The user can optimize all threshold values in the configuration settings in real time.

At the final stage, the integral fluorescence parameters (integral brightness) are calculated for each object. There are two types of measurements: counting pixels and summing their intensity. The total pixel intensity determines the integral brightness of the nucleus. Brightness data is collected in four channels (blue, green, red, and total brightness across all channels) and exported to an Excel file, which ensures compatibility with a wide range of statistical programs for further analysis (Fig. 2c).

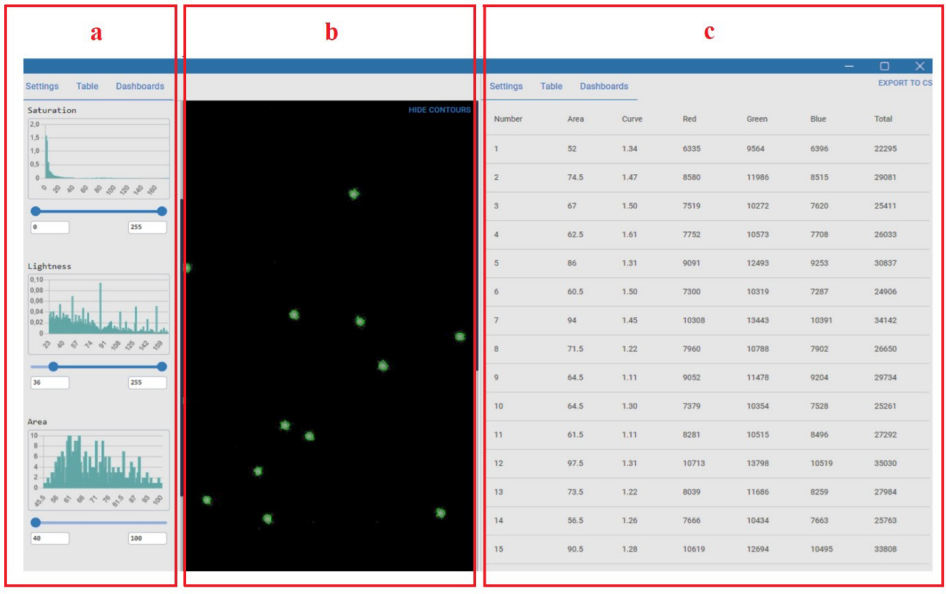

Figure 1. Segmentation of the image of fluorescent particles and intermediate analysis results in the BioDecod program: a – panel of settings; b – the display of particle borders; c – the results of particle parameter analysis in table format.

After the initial data analysis, the next step is to visualize the ratios between the various parameters of the objects using dot plots (Figs. 2a, 2c). The flexibility of the software allows the researcher to independently choose which characteristics will be compared on the X and Y coordinate axes. For example, this can be the ratio of the object's area to its perimeter, the intensity of the glow in individual RGB channels, or the total brightness of the object.

The resulting dot plots serve as the basis for further analysis of distribution of the object's fluorescence intensity. For this purpose, a bar graph is constructed, which clearly demonstrates frequency of occurrence of the objects with a certain level of fluorescence (Fig. 2b, 2d).

An important advantage is the ability to work with the histogram interactively. The user can select a range of fluorescence levels of interest, thereby focusing on a specific subgroup of objects.

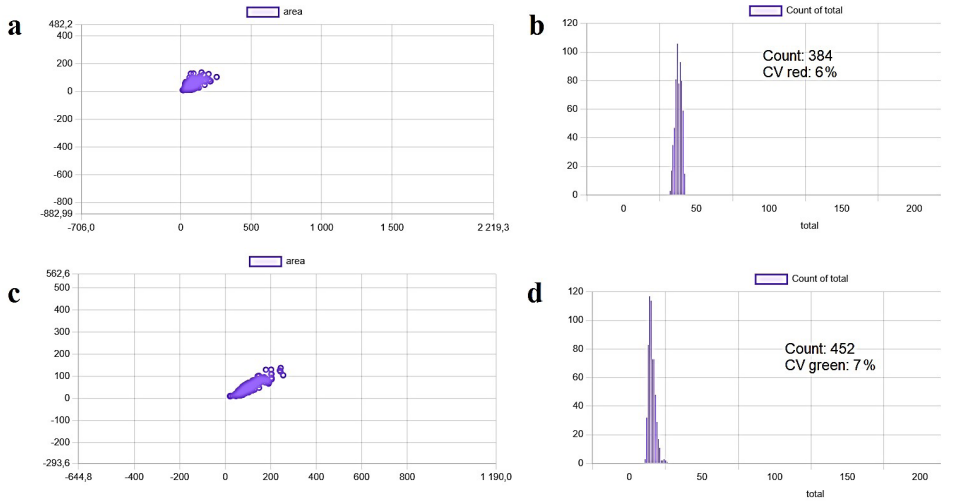

Figure 2. Distribution of particles by fluorescence levels based on ICM, obtained using BioDecod: a – a dot plot of the area versus the fluorescence level of red particles; b – a bar graph of the number of red particles by fluorescence levels; c – a dot plot of the area versus the fluorescence level of green particles; d – a bar graph of the number of green particles by fluorescence levels.

After selecting the target area, the program automatically performs statistical processing of data related to the selected subgroup. The results include the mean value of the fluorescence level for the selected channel – Mean, the standard deviation (measure of dispersion of values) – StdDev, the coefficient of variation (the ratio of the standard deviation to the mean, which makes it possible to estimate relative variability) – CoeffVar, and the number of analyzed objects – Count (Fig. 3).

Thus, the researcher gets the opportunity not only to visually evaluate the distribution of fluorescence but also to obtain quantitative characteristics of the populations of objects interested in. It facilitates the interpretation of the results greatly and allows for more informed conclusions.

Preliminary data processing for comparing the capabilities of BioDecod was also carried out using ImageJ in accordance with the recommendations for working with the program (Ferreira et al. 2012). Image processing included the following

steps. Initially, the image was divided into chroma channels (R, G, and B), resulting in corresponding grayscale images reflecting the chroma intensity of the red, green, and blue colors of the image. Next, the corresponding image was segmented – the green channel for green fluorescent particles and the red channel for red fluorescent particles (Hartig 2013).

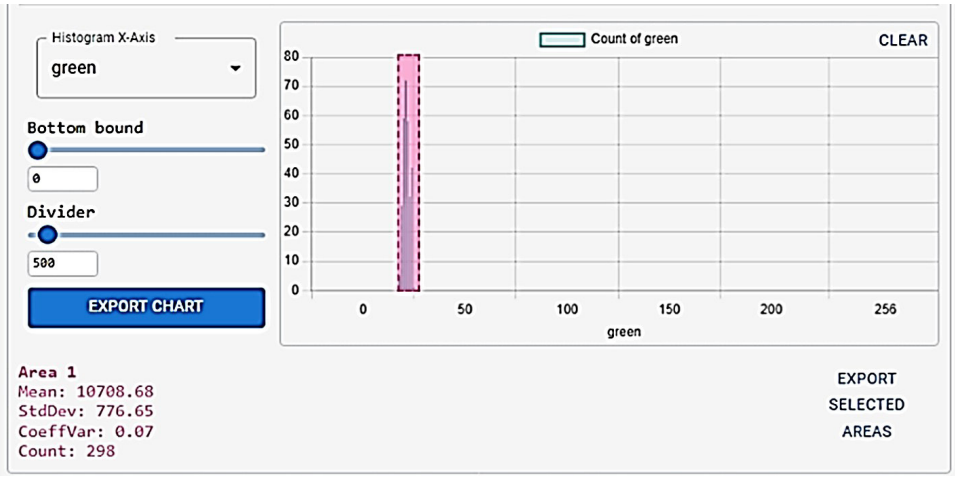

Figure 3. Graphical representation of statistical processing results in the BioDecod application.

For segmentation, a threshold method was used with a custom setting of the background brightness level to 50 relative units for all images. After that, a mask of particle images is created, which must be overlayed on the original grayscale image, and the integral brightness (the sum of the intensity of all pixels of the particle) and the particle area are analyzed. The result of the analysis is an imported tabular file, which is later analyzed in Microsoft Excel to determine the mean integral brightness of the particles and the coefficient of variation of this value. ImageJ does not construct a bar graph with the distribution of the number of particles depending on the intensity, which is its significant disadvantage when processing image cytometry data. We also should note that the entire image processing procedure using ImageJ takes 7 steps, while it is necessary to work with 5 windows in two programs, which is much more difficult compared to BioDecod, where all processing is carried out in a single window, and all settings are available to the user immediately, without creating intermediate files. In addition, in BioDecod user can select areas on bar graph to calculate the statistics of particle parameters only from the user's field of interest.

A similar method of visualization is used on a CytoFlex flow cytometer (Fig. 4). The difference is that to construct the point distribution, the ratio of side or forward scatter of particles and their fluorescence is used in CytoFlex (Fig. 4a, 4c), and the ratio of area or curvature and fluorescence of particles is used in BioDecod.

In flow cytometry, side scatter (SSC) characterizes the internal complexity or granularity of an object's surface, such as the presence of cytoplasmic granules, vesicles, or nuclear structure, while forward scatter (FSC) primarily indicates cell size (Jyoti et al. 2024). Thus, in the BioDecod software, the integral brightness of an object can correspond to the fluorescence level, the object area can correspond to FSC, and the curvature can correspond to SSC.

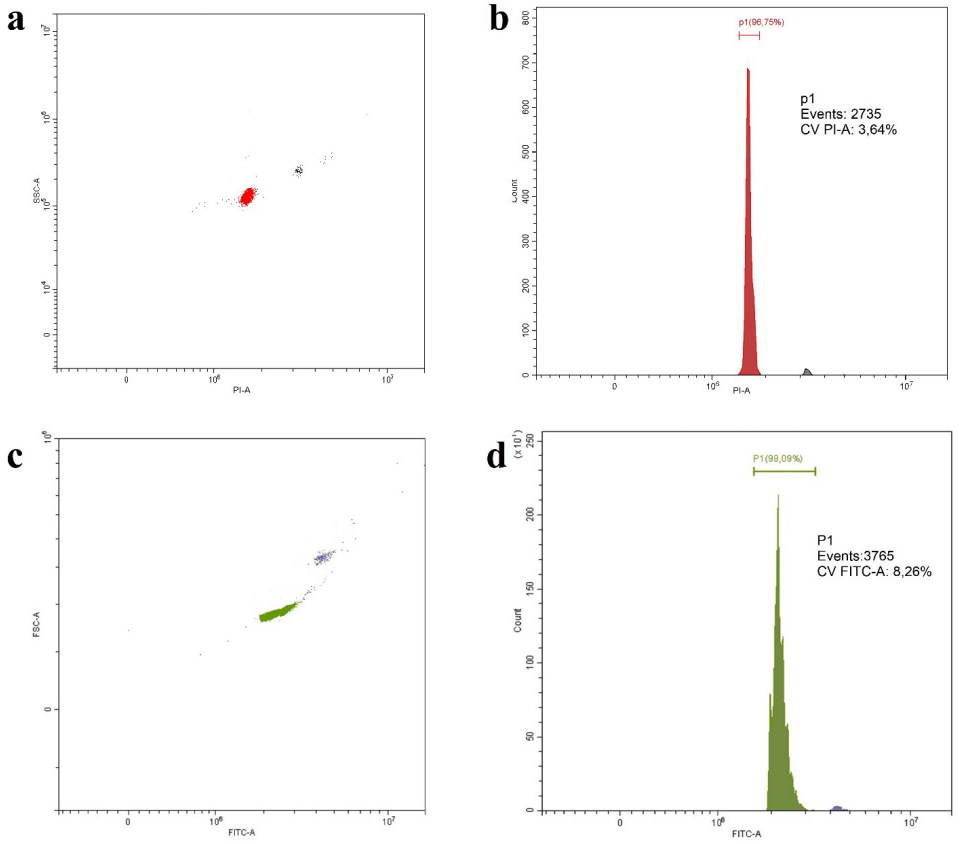

Figure 4. The distribution of particles by fluorescence levels based on FCM, obtained using CytoFLEX: a – a dot plot of the dependence of side scatter on the fluorescence level of red particles; b – a bar graph of the number of red particles by fluorescence levels; c – a dot plot of the dependence of forward scatter on the fluorescence level of green particles; d – a bar graph of the number of green particles by fluorescence levels.

Based on the results of the study of fluorescent particles (Table 1), we concluded that BioDecod image processing is more efficient than ImageJ, which has higher values of the coefficient of variation (CV). When processing the same photographs in BioDecod, CV was 6.31–7.69 % and 14.26–31.1 % in ImageJ. This is due to the

inability to separate particle populations in an image from image artifacts, particle overlays, and incomplete particle images at the borders of photographs when using ImageJ. In this case, to eliminate artifacts, the user would have to select an empirically high value of the ImageJ settings.

The algorithm for determining the borders of objects (in this case, particles) in an image in ImageJ is based on the IsoData method – threshold image detection using iterative selection. The procedure divides the image into an object and a background using an initial threshold, after which the mean values of pixels at or below the threshold and pixels above it are calculated. The means of these two values are calculated, the threshold is increased, and the process is repeated until the threshold is greater than the composite mean (Ridler, Calvard 1978).

Table 1. Comparison of analyses of fluorescent particles using different platforms

	BioDecod, CV, %	**ImageJ, CV, %**	**Average number of particles per photo, pcs.**	**CytoFLEX, CV, %**
Axio imager 2 Microscope				
Red particles	7.15	14.26	85	-
Green particles	6.45	27.47	97	-
ICM-Cytometer Prototype				
Red particles	6.31	23.58	884	-
Green particles	7.69	31.1	887	-
CytoFLEX			**Number of particles per launch, pcs.**	-
Red particles	-	-	2735	3.64
Green particles	-	-	3765	8.26

BioDecod uses threshold segmentation for delimitation of objects (fluorescent particles or nuclei) and the background. The user determines the threshold for outlining borders by adjusting the levels of color balance, chromaticity and brightness. There is also an algorithm for automatic threshold selection – image segmentation based on GMM clustering in HSV space (Yu et al. 2023).

Another advantage of BioDecod compared to ImageJ is the ability to process up to 100 photos simultaneously (ImageJ processes only 1 image file at a time). This is crucial for fast processing of the required amount of data.

A comparison of results of the image cytometry, obtained using the Axio imager 2 fluorescence microscope and the ICM cytometer prototype when processing images of fluorescent particles using BioDecod software, indicates similar data on CV, which is the main criterion for data quality (6.45–7.15 % for Axio imager 2 and 6.31–7.69 % for the ICM cytometer prototype). At the same time, the ICM cytometer prototype is characterized by a significantly higher average number of particles per photograph compared to a fluorescent microscope. This is an indisputable

advantage for obtaining statistically significant data with a smaller total number of photographs. This is due to the wider field of view of the optical system and the larger volume of the sample in the flow cell of the ICM cytometer prototype, compared with the volume located under the cover glass in the case of a fluorescence microscope.

To test the ICM cytometer prototype on real objects, cell nuclei isolated from living plant leaves were used (Table 2). The object illumination power was selected empirically until a linear dependence of the fluorescence level and the DNA content in the nucleus was achieved. The results of flow cytometry were used as reference values of genome sizes.

Table 2. The values of the fluorescence levels of cell nuclei

№	Name of the species, cultivar	Data on the DNA genome content according to FCM, pg	Integral brightness based on ICM, conl. units	CV, %	Correlation of integral brightness and genome size
			The power of the excitation source of the ICM cytometer prototype 30 %		
1	Garden Strawberry (cv. 'Rumba')	0.45 (this paper)	7660	9	0.998
2	Black Rice (cv. 'Aroma D Black rice')	0.955 (this paper)	13186	11	
3	Tomatoe (cv. 'Stupichke')	2.077 (Skaptsov et al. 2024)	27530	7	
4	Corn (cv. 'Owatonna')	5.72 (this paper)	61191	6	
			The power of the excitation source of the ICM cytometer prototype 10 %		
5	Rye (cv. 'Tatiana')	16.19 (this paper)	58302	7	0.933
6	Winter Wheat (cv. unknown)	25 (this paper)	100288	7	
7	Rye (cv. 'Sibir')	32.4 (this paper)	125500	11	
8	*Allium tuberosum*	64.54 (Skaptsov et al. 2024)	160436	6	

Analysis of plants with small genomes (Garden Strawberry 'Rumba', Black Rice 'Aroma D Black rice', Tomato 'Stupichke', Corn 'Owatonna') showed a high correlation between the genome size measured by the FCM method and the integral brightness obtained on an ICM cytometer (R2 = 0.933) at an excitation source power of 30 % for genome size values from 0.45 to 5.72 pg. In the range of 16.19–64.54 pg (from Rye 'Tatiana' to *Allium tuberosum*) and the excitation source power of 10 %, the correlation is slightly lower (R2 = 0.933). This fact indicates the possibility of using integral brightness as an alternative parameter for estimating the genome sizes, especially in cases where direct measurement of DNA content is difficult. The

CV values for most samples are in the range of 6–11 %, which indicates sufficient measurement accuracy. The lowest CV value (6 %) was observed for Corn 'Owatonna' and *Allium tuberosum*, the highest (11 %) – for the rice and Rye 'Siberia'. At the same time, in previous studies conducted using image cytometry, CV values from 0.3 to 21.5 % (Vilhar et al. 2001), as well as 6.2 % (Jónas et al. 2022) were obtained.

For processing microscopy data and images obtained using ICM devices, BioDecod is an alternative to existing tools such as CellProfiler, ImageJ and others due to the fact that the BioDecod software is based on a graphical interface, designed for image cytometry, and does not require multi-stage analysis. The indisputable advantage of BioDecod is its high accuracy, as well as the ability to simultaneously process a large number of images, which is not available for other programs. CellProfiler and ImageJ, on the other hand, are powerful tools, and their functionality goes beyond image cytometry. On the example of BioDecod use cases, we have shown that the ICM cytometer prototype developed provides acceptable results, comparable in accuracy to commercial cytometers and superior to existing software for working with biovisualization datasets for DNA cytometry.

Acknowledgements

The work was supported by the grant of the Russian Science Foundation "Method and device based on DNA cytometry of images for ploidy analysis of agricultural plants and plants of natural flora", No. 24-26-20100.

References

Allalou A, Wählby C (2009) BlobFinder, a tool for fluorescence microscopy image cytometry. Computer Methods and Programs in Biomedicine 94(1): 58–65. https://doi.org/10.1016/j.cmpb.2008.08.006

Broeke J, Pérez JMM, Pascau J (2015) Image Processing with ImageJ. Packt Publishing Ltd., Birmingham, 231 pp.

Chen B, Yin Z, Ng BWL, Wang DM, Tuan RS, Bise R, Ker DFE (2024) Label-free live cell recognition and tracking for biological discoveries and translational applications. npj Imaging 2(1): 41. https://doi.org/10.1038/s44303-024-00046-y

Collins TJ (2007) ImageJ for microscopy. Biotechniques 43(1 suppl): S25–S30.

Ferreira T, Rasban W (2012) ImageJ User Guide IJ 1.46r. Reviewed by Barry DeZonia. https://imagej.net/ij/docs/guide/user-guide.pdf

Fontenete S, Carvalho D, Lourenço A, Guimarães N, Madureira P, Figueiredo C, Azevedo NF (2016) FISHji: New ImageJ macros for the quantification of fluorescence in epifluorescence images. Biochemical Engineering Journal 112: 61–69. https://doi.org/10.1016/j.bej.2016.04.001

Hartig SM (2013) Basic image analysis and manipulation in ImageJ. Current Protocols in Molecular Biology 102(1): 14.15.1–14.15.12. https://doi.org/10.1002/0471142727.mb1415s102

Helmy IM, Abdel Azim AM (2012) Efficacy of ImageJ in the assessment of apoptosis. Diagnostic Pathology 7: 15. https://doi.org/10.1186/1746-1596-7-15

Jónás VZ, Paulik R, Kozlovszky M, Molnár B (2022) Calibration-aimed comparison of image-cytometry-and flow-cytometry-based approaches of ploidy analysis. Sensors 22(18): 6952. https://doi.org/10.3390/s22186952

Jyoti TP, Chandel S, Singh R (2024) Flow cytometry: Aspects and application in plant and biological science. Journal of Biophotonics 17(3): e202300423. https://doi.org/10.1002/jbio.202300423

Kellogg I, Roberts DL, Crespo R (2024) Automated image analysis for detection of coccidia in poultry. Animals 14(2): 212. https://doi.org/10.3390/ani14020212

Kutsev MG, Skaptsov MV, Koltunova AM, Uvarova OV (2024) DNA imaging cytometry in plant analysis: a review. Turczaninowia 27(3): 141–158. https://doi.org/10.14258/turczaninowia.27.3.14 [In Russian]

Li H, Li W, Gao Y, Li J, Zeng X, Lin J, Xie X, Ling T (2024) DNA Image Cytometry for Screening the Carcinogenetic Risk of Oral Potential Malignant Disorders. Journal of Cancer 15(5): 1182–1193. https://doi.org/10.7150/jca.91048

Lippeveld M, Peralta D, Filby A, Saeys Y (2024) SCIP: A scalable, reproducible and open-source pipeline for morphological profiling of image cytometry and microscopy data. Cytometry Part A 105(11): 816–828. https://doi.org/10.1002/cyto.a.24896

Montazerinezhad S, Emamjomeh A, Hajieghrari B (2020) Chromosomal abnormality, laboratory techniques, tools and databases in molecular cytogenetics. Molecular Biology Reports 47(11): 9055–9073. https://doi.org/10.1007/s11033-020-05895-5

Panarin RN, Kutsev MG, Uvarova OV, Koltunova AM (2024) Programma dlia tsitometrii iader kletok [Computer program for cell nuclei cytometry]. Russian Federation Certificate of Registration No. RU 2024687571. [In Russian]

Ridler TW, Calvard S (1978) Picture thresholding using an iterative selection method. IEEE Transactions on Systems, Man, and Cybernetics 8(8): 630–632. https://doi.org/10.1109/TSMC.1979.4310204

Skaptsov MV, Kutsev MG, Smirnov SV, Vaganov AV, Uvarova OV, Shmakov AI (2024) Standards in plant flow cytometry: an overview, polymorphism and linearity issues. Turczaninowia 27(2): 86–104. https://doi.org/10.14258/turczaninowia.27.2.10

Stirling DR, Swain-Bowden MJ, Lucas AM, Carpenter AE, Cimini BA, Goodman A (2021) CellProfiler 4: improvements in speed, utility and usability. BMC Bioinformatics 22(1): 433. https://doi.org/10.1186/s12859-021-04344-9

Vilhar B, Greilhuber J, Koce JD, Temsch EM, Dermastia M (2001) Plant genome size measurement with DNA image cytometry. Annals of Botany 87(6): 719–728. https://doi.org/10.1006/anbo.2001.1394

Vu QD, Graham S, Kurc T, Nhat To MN, Shaban M, Qaiser T, Koohbanani NA, Khurram SA, Kalpathy-Cramer J, Zhao T, Gupta R, Kwak JT, Rajpoot N, Saltz J, Farahani K (2019) Methods for segmentation and classification of digital microscopy tissue im-

ages. Frontiers in Bioengineering and Biotechnology 7: 53. https://doi.org/10.3389/fbioe.2019.00053

Wiesmann V, Franz D, Held C, Münzenmayer C, Palmisano R, Wittenberg T (2015) Review of free software tools for image analysis of fluorescence cell micrographs. Journal of Microscopy 257(1): 39–53. https://doi.org/10.1111/jmi.12184

Xu KF, Jia HR, Wang Z, Feng H-H, Li L-Yi, Zhang R, Durrani S, Lin F, Wu F-G (2023) See the unseen: red-emissive carbon dots for visualizing the nucleolar structures in two model animals and in vivo drug toxicity. Small 19(31): 2205890. https://doi.org/10.1002/smll.202205890

Yu Y, Wang C, Fu Q, Kou R, Huang F, Yang B, Yang T, Gao M (2023) Techniques and challenges of image segmentation: A review. Electronics 12(5): 1199. https://doi.org/10.3390/electronics12051199